

Chapter 1

PRODUCTION OF MULTIPLE ^{87}Rb CONDENSATES AND ATOM LASERS BY RF COUPLING

F. Minardi, C. Fort, P. Maddaloni, and M. Inguscio

INFN – European Laboratory for Non Linear Spectroscopy (L.E.N.S.) – Dipartimento di Fisica dell’Università di Firenze L.go E. Fermi 2, I-50125 Firenze, Italy

INTRODUCTION

One of the major goals in the study of Bose–Einstein condensation (BEC) in dilute atomic gases has been the realization and development of atom lasers. An atom laser may be understood as a source of coherent matter waves. One can extract coherent matter waves from a magnetically trapped Bose condensate. Schemes to couple the atomic beam out of the magnetic trap have been demonstrated [1, 2, 3, 4]. In the experiments of [1, 2] the output coupling is performed by the application of a radio–frequency (rf) field that induces atomic transitions to untrapped Zeeman states. The atom laser described in [3] is based on the Josephson tunnelling of an optically trapped condensate and in [4] a two–photon Raman process is described that allows directional output coupling from a trapped condensate.

Characterizing the output coupler is necessary to understand the atom laser itself. The literature dealing with theoretical descriptions of output couplers for Bose–Einstein condensates has focused both on the use of rf transitions [5, 6, 7, 8] and Raman processes [9].

Rf output coupling is based on single– or multi– step transitions between trapped and untrapped atomic states. As a consequence, a rich phenomenology arises that include the observation of ”multiple” condensates corresponding to atoms in different atomic states. These may display varied dynamical behaviour while in the trap. Also, both pulsed and continuous output–coupled coherent matter beams have been observed. The phenomenology is made even more varied by the possibility of out–coupling solely under gravity and also of magnetically pushed out beams. The apparatus operated by the Florence group [10] offers the

possibility to investigate various aspects of output-coupling achieved by rf transitions of atoms in a magnetically trapped ^{87}Rb .

EXPERIMENTAL PRODUCTION OF THE CONDENSATE

We bring a ^{87}Rb sample to condensation using the now standard technique of combining laser cooling and trapping in a double magneto-optical trap (MOT) and evaporative cooling in a magneto-static trap. Our apparatus had been originally designed for potassium, as presented by C. Fort in this book [11].

Our double MOT set-up consists of two cells connected in the horizontal plane by a 40 cm long transfer tube with an inner diameter of 1.1 cm. We maintain a differential pressure between the two cells in order to optimize conditions in the first cell for rapid loading of the MOT (10^{-9} Torr) while the pressure in the second cell is sufficiently low (10^{-11} Torr) to allow for the long trapping times in the magnetic trap necessary for efficient evaporative cooling.

Laser light for the MOTs is provided by a cw Ti:sapphire laser (Coherent model 899-21) pumped with 8 W of light coming from an Ar^+ laser. The total optical power of the Ti:sapphire laser on the Rb D_2 transition at 780 nm is 500 mW. The laser frequency is locked to the saturated absorption signal obtained in a rubidium vapour cell. The laser beam is then split into four parts each of which is frequency and intensity controlled by means of double pass through an AOM: two beams are red detuned respect to the $F = 2 \rightarrow F' = 3$ atomic resonance and provide the cooling light for the two MOTs. Another beam, resonant on the $F = 2 \rightarrow F' = 3$ cycling transition, is used both for the transfer of cold atoms from the first to the second MOT and for resonant absorption imaging in the second cell. Finally a beam, resonant with the $F = 2 \rightarrow F' = 2$ transition, optically pumps the atoms in the low field seeking $F = 2$, $m_F = 2$ state immediately before switching on the magneto-static trap. 5 mW of repumping light for the two MOTs resonant on the $F = 1 \rightarrow F' = 2$ transition are provided by a diode laser (SDL-5401-G1) mounted in external cavity configuration.

In the first MOT, with 150 mW of cooling light split into three retroreflected beams (2 cm diameter), we can load 10^9 atoms within a few seconds. However, every 300 ms we switch off the trapping fields of the first MOT and we flash on the "push" beam (1 ms duration, few mW) in order to accelerate a fraction of atoms through the transfer tube into the second cell. Permanent magnets placed around the tube generate an hexapole magnetic field that guides the atoms during the transfer. In the

second cell the atoms are recaptured by the second MOT which is operated with six independent beams (diameter=1 cm) each with 10 mW of power. The overall transfer efficiency between the two MOTs is $\sim 30\%$, and after 50 shots we have typically loaded $1.2 \cdot 10^9$ atoms in the second MOT. The final part of laser cooling in the second MOT is devoted to maximizing the density and minimizing the temperature just before loading the magnetic trap. Firstly the atomic density is increased with 30 ms of Compressed-MOT [13] and this is followed by 8 ms of optical molasses to reduce the temperature. Soon after, we optically pump the atoms into the low-field seeking $F = 2$, $m_F = 2$ state by shining the σ^+ -polarized $F = 2 \rightarrow F' = 2$ beam for $200 \mu\text{s}$, together with the repumping light. At this point we switch on the magneto-static trap in the second cell where we perform evaporative cooling of the atoms.

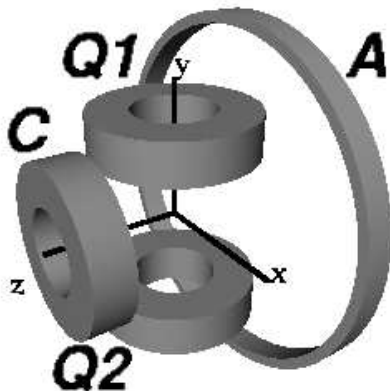


Figure 1.1 4-coils magnetic trap: Q1 and Q2 coils produce the quadrupole field, the curvature coil (C) provides the axial confinement and the antibias coil (A) reduces the bias field thus increasing the radial confinement.

The magneto-static trap is created by passing DC current through 4-coils (see Fig.1.1), which gives rise to a cigar-shaped harmonic magnetic potential elongated along the z symmetry axis (Ioffe-Pritchard type). Our magnetic trap is inspired by the scheme first introduced in [12], but is operated with a higher current. The coils are made from 1/8-inch, water cooled, copper tube. The three identical coils consist of 15 windings with diameters ranging from 3 cm to 6 cm. The fourth coil consists of 6 windings with a diameter of 12 cm. The coils Q1 and Q2 (Fig.1.1) generate a quadrupole field symmetric around the vertical y -axis, and in this direction the measured field gradient is $10 \text{ mT}/(\text{A} \cdot \text{m})$. These two coils

operated together at low current (~ 10 A) also provide the quadrupole field for operation of the MOT. The *curvature* (C) and *antibias* (A) coils produce opposing fields in the z direction. The modulus of the magnetic field during magnetic trapping has a minimum displaced by 5 mm from the center of the quadrupole field (toward the curvature coil) and the axial field curvature is $0.46 \text{ T}/(\text{A}\cdot\text{m}^2)$. The coils are connected in series and fed by a Hewlett Packard 6681A power supply. By means of MOSFET switches we can, however, disconnect coils A and C. The maximum current is 240 A, corresponding to an axial frequency of $\nu_z=13$ Hz for atoms trapped in the $F=2$, $m_F=2$ state. The radial frequency ν_r can be adjusted by tuning $B_b=\min(-B-)$, the bias field at the center of the trap: $\nu_r=(2.18/(B_b[\text{T}])^{1/2})$ Hz. With typical operating values of B_b from 0.14 mT to 0.18 mT, ν_r ranges from 160 Hz to 180 Hz. In addition, a set of three orthogonal pairs of Helmholtz coils provide compensation for stray magnetic fields.

The transfer of atoms from the MOT to the magneto-static trap is complicated by the fact that the MOT (centered at the minimum of the quadrupole field) and the minimum of the harmonic magnetic trap are 5 mm apart. The transfer of atoms from the MOT to the magnetic trap consists of a few steps. We first load the atoms in a purely quadrupole field with a gradient of 0.7 T/m ($I=70$ A), roughly corresponding to the “mode-matching” condition (magnetic potential energy equals the kinetic energy) which ensures minimum losses in the phase-space density. Then we adiabatically increase the gradient to 2.4 T/m by ramping the current to its maximum value $I=240$ A in 400 ms. Finally, the quadrupole potential is adiabatically (750 ms) transformed into the harmonic one by passing the current also through the *curvature* (C) and *antibias* (A) coils, hence moving the atoms 5 mm in the z direction. At the end of this procedure, 30% of atoms have been transferred from the MOT into the harmonic magnetic trap and we start rf forced evaporative cooling with $4 \cdot 10^8$ atoms at 500 μK . We estimate the elastic collision rate to be $\gamma \sim 30 \text{ s}^{-1}$ and this, combined with the measured lifetime in the magnetic trap of 60 s, gives a ratio of “good” to “bad” collisions of ~ 1800 . This is sufficiently high to perform the evaporative cooling and reach BEC.

The rf field driving the evaporative cooling is generated by means of a 10 turn coil of diameter 1-inch placed 3 cm from the center of the trap in the x direction and fed by a synthesiser (Stanford Research DS345). The rf field is first ramped for 20 s with an exponential-like law from 20 MHz to a value which is only 100 kHz above the frequency that empties the trap, $\nu_{rf}^0 = \mu_0 B_b / 2\hbar$. Then a 5 s linear ramp takes the rf closer to ν_{rf}^0 : the BEC transition takes place roughly 5 kHz above ν_{rf}^0 .

We analyse the atomic cloud using resonant absorption imaging. The atomic sample is released by switching off the current through the trapping coils in 1 ms. The cloud then falls freely under gravity and after a delay of up to 25 ms, we flash a probe beam, resonant with the $F = 2 \rightarrow F' = 3$ transition, for $150 \mu\text{s}$ and at one tenth of the saturation intensity. The shadow cast by the cloud is imaged onto a CCD array (pixel size= $24 \mu\text{m}$) with two lenses, giving a magnification of 6. However our resolution is $7 \mu\text{m}$, due to the diffraction limit of the first lens ($f=60 \text{ mm}$, N.A.=0.28). We process three images to obtain the two dimensional column density $\tilde{n}(y, z) = \int n(x, y, z) dx$. The column density is then fitted assuming that $n(x, y, z)$ is the sum of a gaussian distribution corresponding to the uncondensed fraction and an inverted parabola, which is solution of the Gross–Pitaevskii equation in the Thomas–Fermi approximation (condensed fraction). The effect of free expansion, which is trivial for the gaussian part, is taken into account also for the condensate as a rescaling of the cloud radii, according to [14]. The temperature is obtained from the gaussian widths of the thermal cloud.

We observe the BEC transition at a temperature $T_c=200 \text{ nK}$ with $2 \cdot 10^5$ atoms, the peak density n_c being $7 \cdot 10^{19} \text{ m}^{-3}$. The number of condensed atoms shows fluctuations of 20% from shot to shot. We may attribute this to thermal fluctuations of the magnetic trap coils giving rise to fluctuation of the magnetic field.

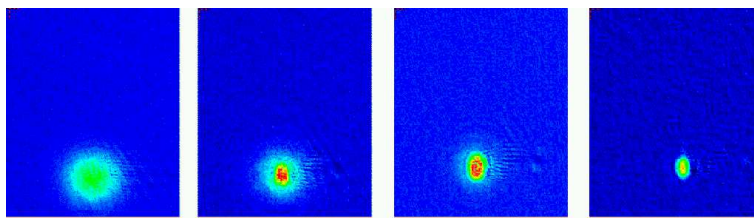


Figure 1.2 Absorption imaging picture of the atomic cloud after a time of flight of 20 ms. From the left to the right the rf ramp was stopped respectively at 0.94 MHz, 0.92 MHz, 0.90 MHz and 0.88 MHz. The symmetric expansion in the first image is typical of a thermal cloud. By further evaporation the high density peak characteristic of the condensate emerges, finally giving rise to a pure condensate.

RADIO-FREQUENCY OUTPUT COUPLING

After producing the condensate in the $F = 2$, $m_F = 2$ state, the same rf field used for evaporation is also employed to coherently transfer

the condensate into different m_F states of the $F = 2$ level. Multistep transitions take place at low magnetic field where the Zeeman effect is approximately linear. This means that the rf field couples all the Zeeman sublevels of $F = 2$. Two of these, $m_F = 2$ and $m_F = 1$, are low-field seeking states and stay trapped. $m_F = 0$ is untrapped and falls freely under gravity, while $m_F = -1$ and $m_F = -2$ are high-field seeking states and are repelled from the trap. Different regimes may be investigated by changing the duration and amplitude of the rf field. The absorption imaging with a resonant beam tuned on the $F = 2 \rightarrow F' = 3$ transition allows us to detect at the same time all Zeeman sublevels of the $F = 2$ state.

It is worth noting that the spatial extent of the condensate results in a broadening of the rf resonance. Due to their delocalization density atoms experience a magnetic field that is non-uniform over their spatial extent. Our condensate is typically $40 \mu\text{m}$ in the axial direction and $4 \mu\text{m}$ in the radial one. The corresponding resonance broadening is of the order of 1 kHz. This means that rf pulses shorter than 0.2 ms interact with all the atomic cloud, while for longer pulses, and sufficiently small amplitudes, only a slice of the condensate will be in resonance with the rf field.

PULSED REGIME

We investigate the regime of “pulsed” coupling characterized by rf pulses shorter than 0.3 ms. In particular, Fig.1.3 shows the effect of a pulse of 10 cycles at ~ 1.2 MHz ($B_b = 0.17$ mT) with an amplitude $B_{rf} = 7 \mu\text{T}$. After the rf pulse, we leave the magnetic trap on for a time Δt and then switch off the trap, thus allowing the atoms to expand and fall under gravity for 15 ms. Pictures from the left to the right correspond to trap times after the rf pulse of $\Delta t = 2, 3, 4, 5$ and 6 ms.

Three distinct condensates are visible (Fig.1.3): we observe that one is simply falling freely in the gravitational field and hence we attribute to the condensate atoms being in the $m_F = 0$ state. The other two condensates initially overlap and then separate. However, we point out that the pictures are always taken after an expansion in the gravitational field. The initial position of the condensate in the trap may be found by applying the equation of motion for free-fall under gravity.

Leaving the magnetic field on for longer times after the rf pulse allows us to identify the condensates in different m_F state by their different center of mass oscillation frequency in the trap. Considering that the images are taken after a free fall expansion of $t_{exp} = 15$ ms, one can deduce the oscillation amplitude in the trap, a , from the observed oscillation

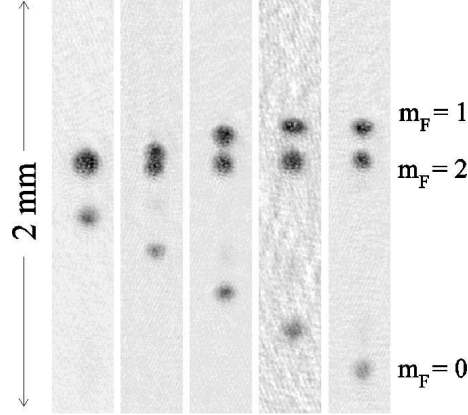


Figure 1.3 Time of flight images of multiple condensates produced by a rf pulse. Taken after 15 ms of free fall, the pictures refer to different evolution times Δt in the magnetic trap, respectively 2,3,4,5 and 6 ms. The $m_F = 2$ condensate is below the center of oscillation of the $m_F = 1$, opposite to what one expects considering the gravitational sagging. This can be explained by the presence of a gradient during the switching off of the magnetic field

amplitude, A , by using the relation

$$A = a\sqrt{1 + \omega_i^2 t_{exp}^2} \quad (1.1)$$

where ω_i is the oscillation frequency for atoms in the $m_F = i$ level.

From Fig.1.3 we note that the position of the center of mass of the condensate in $m_F = 2$ is fixed (at the level of resolution) while the condensate in $m_F = 1$ oscillates at the radial frequency of the corresponding trap potential, with a measured amplitude of $a=8.7 \pm 0.4 \mu\text{m}$. This can be explained by considering the different trapping potentials experienced by the two condensates. The total potential results from the sum of the magnetic and the gravitational potentials, so that the minima for the two states in the vertical direction are displaced by $\Delta y=g/\omega_r^2$ (“sagging”). With the experimental parameter of Fig.1.3 ($\omega_r = 2\pi(171 \pm 4 \text{ Hz})$ for atoms in $F = 2$, $m_F = 2$ state) Δy equals $8.5 \pm 0.4 \mu\text{m}$. This is in very good agreement with the measured center of mass oscillation amplitude. The $m_F = 1$ condensate is produced at rest in the equilibrium position of the $m_F = 2$ condensate and begins to oscillate around its own potential minimum with an amplitude equal to Δy .

Fig.1.3 shows the situation where the rf pulse is adjusted to equally populate the two trapped states, $m_F = 1$ and $m_F = 2$. In general, the

relative population in different Zeeman sublevels can be determined by varying the duration of the rf pulse. This is clearly illustrated in Fig.1.4, where the relative population of the $m_F = 2, 1$ and 0 condensates are shown as a function of the pulse duration.

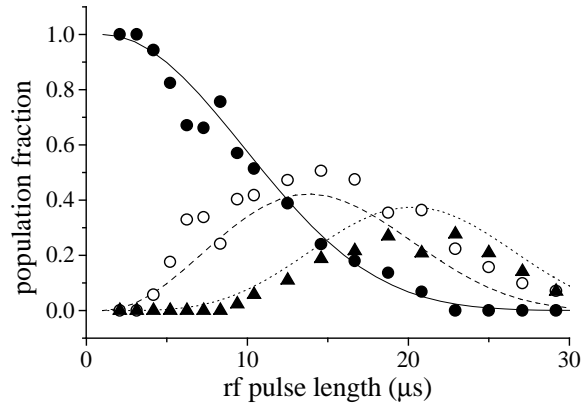


Figure 1.4 Measured population fraction of $m_F = 2$ (solid circle), $m_F = 1$ (open circle) and $m_F = 0$ (triangle) states as a function of rf pulse duration. The curves correspond to the calculated Rabi oscillations of the relative population in $m_F = 2$ (solid line), $m_F = 1$ (dashed line) and $m_F = 0$ (dotted line).

The theoretical curves, calculated for a Rabi frequency of 26 kHz corresponding to the amplitude of our oscillating rf magnetic field $B_{rf} = 3.6 \mu\text{T}$, are shown together with the experimental data. The population of each Zeeman state is calculated by solving the set of the Bloch equation in the presence of an external rf coupling field. These results clearly show that we can control in a reproducible way the relative populations of the multiple condensates. It is worth noting that the use of a static magnetic trap allows a straightforward explanation of the phenomenon; similar investigations recently reported for a time-dependent TOP trap [15] show that the theory is more complicated in presence of a time varying magnetic field.

The $m_F = -1, -2$ sublevels are also populated by rf induced multi-step transitions. However, these condensates are quickly expelled by the magnetic potential and the effect can be observed for shorter times after the rf pulse. This is evident in the image in Fig.1.5 which is taken under the same conditions of Fig.1.3 but with a shorter time ($\Delta t = 1.5$ ms) in

the magnetic trap. As expected, in addition to the free-falling $m_F = 0$ condensate atoms coupled-out simply by gravity, an elongated cloud appears, corresponding to atoms in the high-field seeking states that are repelled from the trap.

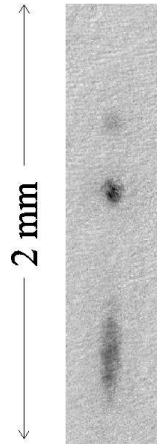


Figure 1.5 Absorption imaging of the multicomponent condensate produced by a rf pulse. The magnetic trap was on for 1.5 ms after the rf pulse and the picture was taken after 20 ms of free expansion.

CW ATOM LASER

Continuously coupling atoms out of a Bose condensate with resonant rf radiation was first proposed by W. Ketterle et al. [1]. In their paper on the rf output coupler they discuss this scheme and point out the necessity to have a very stable magnetic field. I. Bloch et al. [2] realized a cw atom laser based on rf output coupling using an apparatus with a very well controlled magnetic field. They placed a μ -metal shield around the cell where the condensate forms, achieving residual fluctuations below 10^{-8} T.

We explored the regime of continuous coupling by leaving the rf field on for at least 10 ms. In this case we observed a stream of atoms escaping from the trap (Fig.1.6). The experimental configuration is similar to the one described in [2], except for the fact that our apparatus is not optimized to minimize magnetic field fluctuations, that are at the level of 10^{-6} T. Nevertheless, our observation demonstrate that these fluctuations do not prevent the operation of a cw atom laser.

Fig.1.6 shows an absorption image taken after an rf pulse 10 ms long with an amplitude $B_{rf}=0.36 \mu\text{T}$. The first picture corresponds to the temperature of the rubidium atoms being above the critical temperature (T_c) for condensation. In this case a very weak tail of atoms escaping from the magnetically trapped cloud is observed. Decreasing the temperature below T_c (second picture of Fig.1.6) the beam of atoms leaving the trap becomes sharper and more collimated.

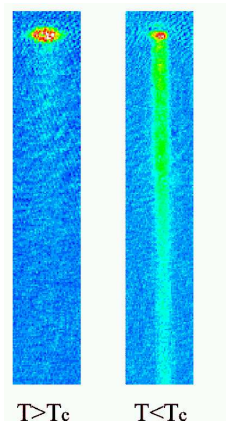


Figure 1.6 Absorption imaging of the atom laser obtained applying a rf field for 10 ms and illuminating the atoms 5 ms after switching off the trap.

We have demonstrated a cw atom laser. However, the fluctuations in our magnetic field strongly influences not only the reproducibility but also the quality of the extracted beam. The high magnetic field stability achieved by the Munich group allowed the measurement of the spatial coherence of a trapped Bose gas [16, 17] by observing the interference pattern of two matter waves out-coupled from the condensate using a rf field composed of two frequencies.

CONCLUSIONS

We have illustrated the rich phenomenology arising from the interaction of an rf field with a ^{87}Rb condensate originally in the $F = 2, m_F = 2$ state. We have shown that condensates can be produced in each of the five Zeeman sublevels and that the relative populations can be controlled by varying the duration and amplitude of the rf pulse. We investigated the behaviour of both trapped and untrapped condensates as a function of the time in the magnetic trap. At short times we recorded the dif-

ferent behaviour between the atoms output-coupled under gravity only ($m_F = 0$), and those with an additional impulse due to the magnetic field ($m_F = -1, -2$). We have also produced a cw atom laser by simply increasing the time duration of the rf pulse. In our apparatus no particular care is devoted to the shielding of unwanted magnetic field. The stability and homogeneity requirements seem to be less stringent than those predicted in the pioneering work of [1] and of those of the magnetic field implemented by the original cw atom laser apparatus [2]. This could make the cw atom laser based on rf out-coupling more generally accessible. Most of the observed phenomena may be understood using a simple theoretical model; a more detailed and complete description of the multicomponent condensate should take into account also the mean field potential and interaction between different condensates.

Future applications of the experimental set-up we are currently operating can be foreseen, for instance for the study of collective excitations induced by the sudden change in the atom number. The interaction between condensates in different internal states may possibly be investigated as well as time-domain matter-wave interferometers using a sequence of rf pulses.

Acknowledgments

We would like to thank M. Prevedelli for his contribution in setting up the experiment. This work was supported by the INFM "Progetto di Ricerca Avanzata" and by the CNR "Progetto Integrato". We would like to thank also D. Lau for careful reading of the manuscript.

References

- [1] Mewes, M. -O., Andrews, M. R., Kurn, D. M., Durfee, D. S., Towsend, C. G., and Ketterle, W. (1997) An output coupler for Bose condensed atoms *Phys. Rev. Lett.* **78**: 582
- [2] Bloch, I., Hänsch, T. W. and Esslinger, T. (1999) An Atom Laser with a cw Output Coupler *Phys. Rev. Lett.* **82**: 3008.
- [3] Anderson, B. P., and Kasevich, M. A. (1998) Macroscopic Quantum Interference from Atomic Tunnel Arrays *Science* **282**: 1686.
- [4] Hagley, E. W., Dung, L., Kozuma, M., Wen, J., Helmerston, K., Rolston, S. L., and Phillips, W. D. (1999) A well Collimated Quasi-Continuous Atom Laser *Science* **283**: 1706.
- [5] Naraschewski, M., Schenzle, A., and Wallis, H. (1997) Phase diffusion and the output properties of a cw atom-laser *Phys. Rev. A* **56**: 603.

- [6] Ballagh, R. J., Burnett, K., and Scott, T. F. (1997) Theory of an Output Coupler for Bose-Einstein Condensed Atoms *Phys. Rev. Lett.* **78**: 1607.
- [7] Steck, H., Naraschewski, M., and Wallis, H. (1998) Output of a pulsed Atom Laser *Phys. Rev. Lett.* **80**: 1.
- [8] Band, Y. B., Julienne, P. S., and Trippenbach, M. (1999) Radio-frequency output coupling of the Bose-Einstein condensate for atom lasers *Phys. Rev. A* **59**: 3823.
- [9] Edwards, M., Griggs, D. A., Holman, P.L., Clark, C. W., Rolston, S. L., and Phillips, W. D. (1999) Properties of a Raman atom-laser output coupler *J. Phys. B* **32**: 2935.
- [10] Fort, C., Prevedelli, M., Minardi, F., Cataliotti, F. S., Ricci, L., Tino, G. M., and Inguscio, M. (2000) Collective excitations of a ^{87}Rb Bose condensate in the Thomas Fermi regime *Eur. Phys. Lett.* **49**: 8.
- [11] Fort, C. Experiments with potassium isotopes in this Volume.
- [12] Esslinger, T., Bloch, I., and Hänsch, T. W. (1998) Bose-Einstein condensation in a quadrupole-Ioffe-configuration trap *Phys. Rev. A* **58**: R2664.
- [13] Petrich, W., Anderson, M. H., Ensher, J. R., and Cornell, E. A. (1994) Behavior of atoms in a compressed magneto-optical trap *J. Opt. Soc. Am. B* **11**: 1332.
- [14] Castin, Y., and Dum, R. (1996) Bose-Einstein Condensates in Time-Dependent Traps *Phys. Rev. Lett.* **77**: 5315.
- [15] Martin, J. L., McKenzie, C. R., Thomas, N. R., Warrington, D. M., and Wilson, A. C. Production of two simultaneously trapped Bose-Einstein condensates by RF coupling in a TOP trap cond-mat/9912045.
- [16] Esslinger, T., Bloch, I., Greiner, M., and Hänsch, T. W. Generating and manipulating Atom Lasers Beams in this Volume.
- [17] Bloch, I., Hänsch, T. W., and Esslinger, T. (2000) Measurement of the spatial coherence of a trapped Bose gas at the phase transition *Nature* **403**: 166.